1-1-2020

Striatal Acetylcholine Helps to Preserve Functional Outcomes in a Mouse Model of Stroke

Daniela F. Goncalves
Robarts Research Institute

Monica S. Guzman
Robarts Research Institute

Robert Gros
Robarts Research Institute

André R. Massensini
Universidade Federal de Minas Gerais

Robert Bartha
Robarts Research Institute, rbartha@robarts.ca

See next page for additional authors

Citation of this paper:

Goncalves, Daniela F.; Guzman, Monica S.; Gros, Robert; Massensini, André R.; Bartha, Robert; Prado, Vania F.; and Prado, Marco A.M., "Striatal Acetylcholine Helps to Preserve Functional Outcomes in a Mouse Model of Stroke" (2020). *Medical Biophysics Publications*. 610.
https://ir.lib.uwo.ca/biophysicspub/610

Authors

Daniela F. Goncalves, Monica S. Guzman, Robert Gros, André R. Massensini, Robert Bartha, Vania F. Prado, and Marco A.M. Prado

Striatal Acetylcholine Helps to Preserve Functional Outcomes in a Mouse Model of Stroke

Daniela F. Goncalves[1,2,*], Monica S. Guzman[1,3,*], Robert Gros[1,3], André R. Massensini[2], Robert Bartha[1,4], Vania F. Prado[1,3,5] (iD), and Marco A. M. Prado[1,3,5] (iD)

Abstract

Acetylcholine (ACh) has been suggested to facilitate plasticity and improve functional recovery after different types of brain lesions. Interestingly, numerous studies have shown that striatal cholinergic interneurons are relatively resistant to acute ischemic insults, but whether ACh released by these neurons enhances functional recovery after stroke is unknown. We investigated the role of endogenous striatal ACh in stroke lesion volume and functional outcomes following middle cerebral artery occlusion to induce focal ischemia in striatum-selective vesicular acetylcholine transporter-deficient mice (stVAChT-KO). As transporter expression is almost completely eliminated in the striatum of stVAChT-KO mice, ACh release is nearly abolished in this area. Conversely, in other brain areas, VAChT expression and ACh release are preserved. Our results demonstrate a larger infarct size after ischemic insult in stVAChT-KO mice, with more pronounced functional impairments and increased mortality than in littermate controls. These changes are associated with increased activation of GSK-3, decreased levels of β-catenin, and a higher permeability of the blood–brain barrier in mice with loss of VAChT in striatum neurons. These results support a framework in which endogenous ACh secretion originating from cholinergic interneurons in the striatum helps to protect brain tissue against ischemia-induced damage and facilitates brain recovery by supporting blood–brain barrier function.

Keywords

VAChT, ischemia, stroke, blood–brain barrier, mice, gait, GSK-3

Received July 28, 2020; Revised August 27, 2020; Accepted for publication August 31, 2020

Striatal cholinergic interneurons (CINs) represent the major source of cholinergic innervation in the striatum. They are tonically active and have dense and extensive axonal arborization that covers most of the striatum (Kawaguchi et al., 1995). CINs represent only a small fraction of the total neuronal population in the striatum (1%–3% in rodent and up to 20% in primates), but provide multiple levels of modulation for striatal function (Kljakic et al., 2017; Prado et al., 2017).

Numerous studies have shown that striatal CINs are relatively resistant to acute ischemic insults. For instance, 20 to 30 min of middle cerebral artery occlusion (MCAO) leads to substantial loss of projection medium spiny neurons, while CINs are relatively preserved, possibly due to their intrinsic membrane properties (Andsberg et al.,

[1]Robarts Research Institute, The University of Western Ontario, London, Canada
[2]Neuroscience Centre, Department of Physiology and Biophysics, Universidade Federal de Minas Gerais, Belo Horizonte, Brazil
[3]Department of Physiology and Pharmacology, The University of Western Ontario, London, Canada
[4]Department of Medical Biophysics, The University of Western Ontario, London, Canada
[5]Department of Anatomy and Cell Biology, The University of Western Ontario, London, Canada

*These authors contributed equally to this work.

Corresponding Author:
Marco A. M. Prado, Robarts Research Institute, The University of Western Ontario, 1151 Richmond St. N, London, ON N6A 5B7, Canada.
Email: mprado@robarts.ca

2001; Katchanov et al., 2003; Deng et al., 2008). Recordings from CINs after ischemia indicate that 24 hr after ischemia, their firing properties return to normal levels, suggesting that they are able to sustain the release of acetylcholine (ACh; Deng et al., 2008).

Noteworthy, ACh has been shown to facilitate cortical plasticity and improve functional recovery after physical lesions in the motor cortex (Conner et al., 2003, 2005). Therefore, the activity of CINs could contribute to functional recovery in the striatum after ischemia/reperfusion. Pharmacological studies suggest that stimulation of $\alpha 7$ nicotinic acetylcholine receptors ($\alpha 7$nAChR) attenuates cell death and inflammation in the hippocampus after experimental hemorrhagic ischemia (B. Sun et al., 2011; Krafft et al., 2012, 2013) and also reduces brain edema and preserves blood–brain barrier (BBB) integrity after intracerebral blood infusion (Krafft et al., 2012, 2013). Similar beneficial effects are observed with cholinesterase inhibitors in animal models (Lorrio et al., 2007). Furthermore, results from a Phase II clinical trial showed that acute ischemic stroke patients treated with cholinesterase inhibitors have improved functional recovery (Barrett et al., 2011).

To investigate the role of endogenous striatal ACh secreted from CINs on stroke outcome, we used MCAO to induce focal ischemia in mice with striatum-selective genetic deficiency in the vesicular acetylcholine transporter (VAChT$^{\text{D2Cre-flox/flox}}$: herein referred as stVAChT-KO; Guzman et al., 2011). VAChT is responsible for loading ACh into synaptic vesicles (Prado et al., 2013) and is essential for ACh storage and release (Prado et al., 2006; de Castro, De Jaeger, et al., 2009; Lima et al., 2010). Changes in VAChT expression/function directly regulate the amount of ACh released from nerve terminals (Van der, 2003; Prado et al., 2006; de Castro, De Jaeger, et al., 2009; Lima et al., 2010; Guzman et al., 2011; Martyn et al., 2012; Kolisnyk et al., 2013a; Sakae et al., 2015; Sugita et al., 2016; Kolisnyk et al., 2017; Janickova et al., 2017a). As VAChT expression is almost completely eliminated in the striatum of stVAChT-KO mice, ACh release is nearly abolished in this area; conversely in other brain areas VAChT expression and ACh release are preserved (Guzman et al., 2011).

The present experiments indicate impaired recovery after ischemia in VAChT-deficient mice, with increased neuronal damage, and worse functional outcomes. VAChT-deficient mice have increased permeability of the BBB, suggesting that ACh release from striatal cholinergic neurons plays an important role to preserve brain function after ischemia.

Materials and Methods

Animals

All animal procedures were conducted in accordance with the ARRIVE guidelines and conformed to the Canadian Council of Animal Care guidelines for the care and use of animals with an approved animal protocol from the Institutional Animal Care and Use Committees at The University of Western Ontario (protocol number 2016-104). Animals were housed in groups of three or four per cage in a temperature-controlled room with 14:10 light–dark cycles. Food and water were provided for *ad libitum* consumption. Mice were randomly assigned to experimental groups and the experimenter was kept blind regarding genotypes.

Adult male VAChT$^{\text{D2-Cre-flox/flox}}$ mice and control VAChT$^{\text{flox/flox}}$ littermates (3–6 months) were used for this study. VAChT$^{\text{D2-Cre-flox/flox}}$ mice were generated by crossing VAChT$^{\text{flox/flox}}$ with the D2-Cre mouse line as previously described (Guzman et al., 2011).

Magnetic resonance imaging (MRI) measurements were performed 24 hr after surgery and behavioral testing was performed before and 7 days after stroke. Sham-operated mice were scanned and subjected to behavioral tests with the same time intervals as post-ischemic mice. For surgery and MRI recordings, mice were anesthetized with 4% isoflurane (in a NO_2/O_2 70/30% mixture), and maintenance was achieved by inhalation of 1.5% isoflurane. Body temperature was maintained at 37.0 ± 0.5°C as previously described (Beraldo et al., 2013; McVicar et al., 2014).

Stroke Model

Experimental stroke was induced by up to 60 min occlusion of the left middle cerebral artery (MCA) as previously described (Longa et al., 1989; Belayev et al., 1999; Pham et al., 2011; Beraldo et al., 2013). Under an operating microscope, a silicon rubber-coated monofilament (702256PK; Doccol Company, Redlands, CA, USA) was inserted through the left common carotid artery into the internal carotid artery to occlude the MCA. Sham-operated animals underwent the same procedure with the exception of the advancement of the filament to occlude the cerebral artery. After filament insertion, mice were removed from anesthesia and allowed to move freely under a heat lamp. After ischemia, mice were anesthetized again and the filament was quickly removed. To maintain hydration, saline was injected intraperitonially (IP) 1 hr after surgery. Saline injection was repeated daily for 3 days after surgery. To determine the efficacy of the ischemic procedure, animals were evaluated neurologically at 1 hr, 24 hr, and 48 hr after surgery according to the following scores modified from the 5-point Bederson scale (Bederson et al., 1986): 0 = *no deficit*; 1 = *mild forelimb weakness*; 2 = *severe forelimb weakness, consistent turns to the deficit side when lifted by the tail*; 3 = *compulsory circling*; 4 = *unconsious*; and 5 = *dead*. Only mice with a score of 2 or 3 were used in the experiments.

Heart rate data were obtained at baseline, during ischemia and 24 hr after surgery in conscious mice using the CODA computerized noninvasive system (Kent Scientific, Torrington, CT, USA). Rectal temperature was monitored by a Homeothermic blanket control unit (Harvard Apparatus, Holliston, MA, USA). Arterial blood samples (via cardiac puncture under isoflurane anesthesia) were taken 24 hr after surgery and analyzed for pH and glucose using a blood analyzer (ABL-725, Radiometer, Copenhagen, Denmark). Measurement of perfusion using laser Doppler (Beraldo et al., 2013; McVicar et al., 2014) demonstrated that MCAO decreased perfusion by $86 \pm 3\%$ on average compared to the perfusion before surgery ($N = 4$).

Behavioral Testing

Behavioral tests were performed in post-ischemic and sham-operated mice before and 7 days after stroke. The adhesive removal test was used to determine functional recovery. This test is sensitive to unilateral somatosensory dysfunction (Bouet et al., 2009). A small adhesive-backed paper was used as tactile stimuli on the distal-radial region of the wrist of each forelimb. The time each animal took to perceive and remove the tape was recorded for a maximum of 3 min. Three trials were conducted in a single day and averaged as previously described (Beraldo et al., 2013).

Locomotor activity was measured using an automated activity monitor as previously described (Prado et al., 2006; de Castro, Pereira, et al., 2009; Martyn et al., 2012). Experiments were performed between 10:00 and 16:00 hr in the light cycle. Gait was measured using the Catwalk XT system by Noldus (Leesburg, VA, USA), as previously described (Vandeputte et al., 2010; Janickova et al., 2017b). The following parameters were recorded and used for analysis: print area (surface area of the complete print), intensity of the paws (signal depends on the degree of contact between a paw and the glass plate and increases with increasing pressure), swing speed (speed of the paw during swing), and stride length (the distance between successive placements of the same paw). This test was performed prior to the induction of stroke and 7 days after. Catwalk analysis was performed on a minimum of four normal step sequence patterns in each of three uninterrupted runs per animal. The values were expressed relative to the control mean (stroke/sham-operated mean).

Magnetic Resonance Imaging

An Agilent (Agilent, Palo Alto, CA, USA) 9.4 T small animal horizontal bore MRI system was used to acquire images of the mouse brain 24 hr after MCAO. Anesthesia was induced using 4% isoflurane in oxygen and maintained with 1.5% to 2.5% isoflurane in oxygen. The mouse was held in place on a custom-built MRI-compatible stage, and the head was positioned using a bite bar and surgical tape to limit motion due to respiration. A rectal probe was used to monitor the temperature, and respiration was monitored with a sensor pad connected to a pressure transducer placed on the thoracic region. Body temperature was maintained at 36.9 to 37.1°C throughout imaging by blowing warm air over the animal using a model 1025 small-animal monitoring and gating system (SA Instruments Inc., Stony Brook, NY, USA). Two imaging sequences were used to visualize tissue damage due to ischemia: (a) a T_2-weighted two-dimensional fast spin echo sequence (TE $=45$ ms, TR $= 3,000$ ms, FOV $= 19.2 \times 19.2$ mm^2, 31 slices, slice thickness $= 500$ μm, acquisition matrix 128×128) and (b) a T1 three-dimensional balanced steady state free precession sequence (TE $= 3.7$ ms, TR $= 7.4$ ms, FOV $= 19 \times 16 \times 13$ mm^3, acquisition matrix $= 154 \times 132 \times 102$). Infarct volume was measured by manual tracing of the hyperintense tissue in each slice of the T_2 images using ImageJ software. Analysis was performed by D. F. G. blinded to the genotypes as we previously described (Beraldo et al., 2013).

Western Blot

Immunoblotting was performed as described elsewhere (Kolisnyk et al., 2013b). Primary antibodies used for immunoblotting: anti-phospho-Akt Ser473 (Cell Signaling, Cat#9271), anti-total-Akt (Cell Signaling, Cat#9272), phospho-GSK3b Ser9 (Cell Signaling, Cat#9336), GSK3b (Cell Signaling, Cat#9315), phospho-GSK3b Tyr216 (Abcam, Cat# ab75745), and anti-beta-catenin (Abcam, Cat# ab6302). Loading control used was anti-β-actin (1:25000, Sigma, Cat#A3854) and secondary antibodies were sheep anti-mouse HRP (1:5000, Cat#SAB3701095, Sigma) and goat anti-rabbit HRP (1:10000, Cat#170-6515, BioRad). Proteins were visualized using chemiluminescence on FluoroChemQ chemiluminescent exposure system (Alpha Innotech; GE Healthcare, London, ON, Canada) or ChemiDoc MP Imaging System (BioRad) and analyzed using their respective software (Alpha Innotech and Image Lab).

Histology

Brains were removed and sectioned coronally into 2-mm-thick slices 24 hr after stroke. The slices were stained with 2% triphenyltetrazolium chloride (TTC) solution at 37°C for 15 min, followed by fixation with 10% formalin neutral buffer solution (pH 7.4) (Benedek et al., 2006). The infarct areas were traced and quantified as percentage of contralateral hemisphere using an Image-J system.

Unstained areas (pale color) were defined as ischemic lesions.

To evaluate BBB integrity, diffusion of IgG into the brain parenchyma was determined. Brain sections were incubated with 0.3% H_2O_2 for 30 min to abolish endogenous peroxidase activity. After several rinses with tris-buffered saline, the sections were blocked with tris-buffered saline-bovine serum albumin for 1 hr, and then incubated with goat anti-mouse IgG conjugated with horseradish peroxidase for 1 hr. To reveal IgG, the VECTOR NovaRED peroxidase substrate kit was used (VECTOR Laboratories, Inc., Burlingame, CA, USA). The intensity was measured in both hemispheres and quantified as a ratio (ipsilateral/contralateral) using ImageJ software.

Statistical Analysis

All data are expressed as mean $\pm$ *SEM*. Sigmastat 3.5 software was used for statistical analysis. Comparison between two experimental groups was done by Student's *t* test or Mann–Whitney Rank Sum test when the data failed the Normality test. Comparisons for multiple groups were performed using analysis of variance (ANOVA) or repeated measures ANOVA followed by a Tukey *post hoc* test. Catwalk outcomes of VAChT[D2-Cre-flox/flox] and control mice were compared for each paw using a one-tailed nonparametric Mann–Whitney test. Survival curves were analyzed using a log-rank test. Differences were considered to be statistically significant when $p < .05$.

Results

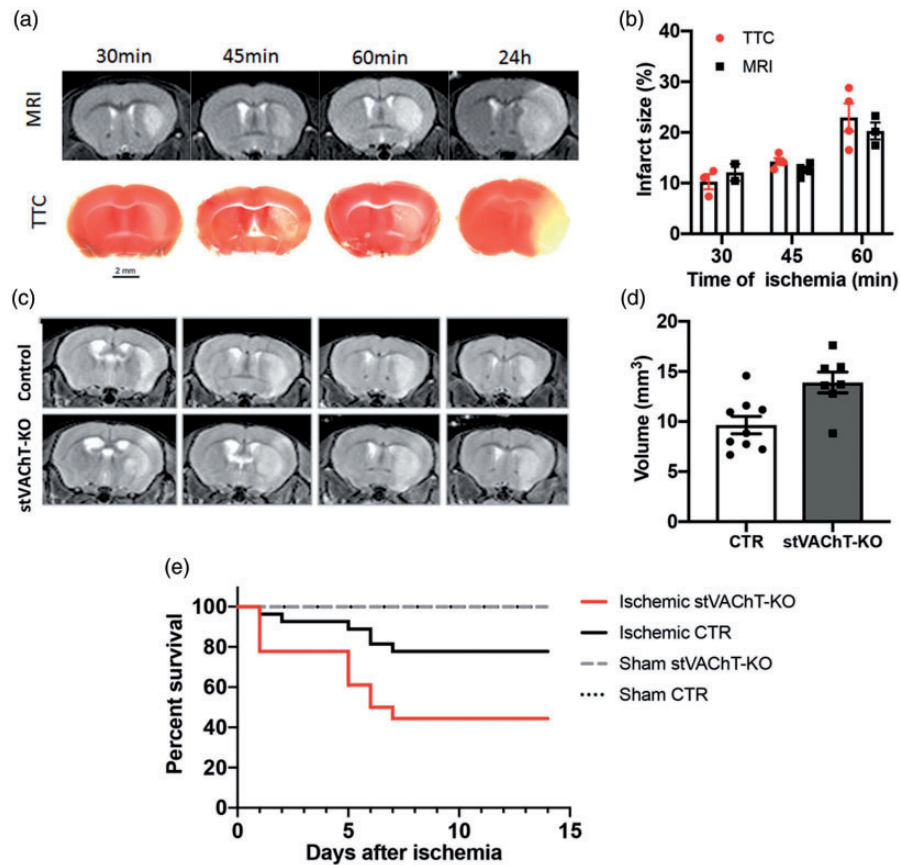### Infarct Area and Mortality Rate Are Increased in stVAChT-KO Mice After Ischemia-Reperfusion

We used the MCAO model (Longa et al., 1989) to induce mild brain ischemia in mice. Our initial experiment was designed to determine the experimental conditions that would confine brain damage mainly to the striatum that could be confidently assessed by MRI. We tested wild-type mice at three different occlusion times: 30, 45, and 60 min and after 24 hr of reperfusion, we determined lesion location and volume using T_2-weighted MRI (Figure 1A, top) and TTC staining (Figure 1A, bottom). For comparison, we also tested 24-hr occlusion with no reperfusion (Figure 1A). As expected, 24-hr occlusion led to extensive cortical and striatal injury that could be easily detected by both TTC and MRI. TTC staining analysis showed that after 24-hr reperfusion, lesions produced by 30-, 40-, and 60-min occlusion showed a respective increase in size expressed in percentage of contralateral hemisphere volume (Figure 1B, 30 min: $10.3 \pm 1.5\%$, 45 min: $14.3 \pm 0.7\%$, 60 min: $22.9 \pm$

2.8%) but, even with the longest duration of MCAO, the cortex was mostly spared and tissue damage was mainly restricted to the striatum (Figure 1A). Importantly, estimation of lesion size (relative to contralateral hemisphere) using T_2-weighted MRI images (Figure 1B, 30 min: $12.1 \pm 1.7\%$, 45 min: $12.6 \pm 0.6\%$, 60 min: $20.3 \pm 1.7\%$) were very similar to those obtained using TTC staining (two-way ANOVA effect of time $F(1.040, 7.281) = 19.18$, $p = .0028$), indicating that 24 hr after reperfusion T_2-weigthed MRI could be used to accurately measure the extent and location of stroke lesions in mice. Thus, for the following experiments designed to examine functional recovery, injury size was measured using T_2-weighted MRI images collected 24 hr after 60 min of MCAO.

The role of striatal ACh on stroke outcome was investigated using stVAChT-KO mice (Guzman et al., 2011). stVAChT-KO and littermate controls (VACh[flox/flox]) were submitted to 60 min MCAO and 24 hr after reperfusion, brain lesions and physiological parameters were measured. We observed that absolute infarct size in stVAChT-KO mice was 30% larger than in littermate controls (Figure 1C and D, controls: 9.6 ± 0.9 mm^3 $N = 9$; stVAChT-KO: 13.9 ± 1.0 mm^3 $N = 7$; unpaired Student's *t* test with Welch's correction; $t(12.6) = 3.15$, $p = .008$), and sham-operated VAChT-mutant and control mice showed no signs of stroke. Furthermore, while 78% of control mice survived past the first week of stroke, surprisingly the survival rate of stVAChT-KO mice was 44%, almost two-fold lower than that of littermate controls, while the survival rate of sham-operated VAChT-mutant and control mice was 100% (Figure 1E; log-rank Mantel-Cox test; MCAO-controls $N = 27$; MCAO-stVAChT-KO $N = 18$, sham-controls $N = 3$, sham-stVAChT-KO $N = 7$, $p < .05$). To note, physiological parameters such as heart rate, arterial blood pH, oxygen saturation, temperature, glucose, pO2, and pCO2, measured 24 hr following ischemic insult were not significantly different between stVAChT-KO mice and littermate controls (Table 1), suggesting that changes in these parameters did not contribute to increased mortality. Taken together, these results indicate that stroke injury in VAChT-mutant mice was significantly worse when compared to littermate controls, which seem to contribute to increased mortality.

Gait and Sensorimotor Deficits Are More Pronounced in stVAChT-KO Mice After Ischemia-Reperfusion

Seven days after MCAO, sham-operated and ischemic stVAChT-KO and littermate controls were subjected to functional tests, to evaluate functional outcomes after striatal ischemia. Locomotor activity measured for 2 hr on an automated locomotor box showed that both stVAChT-KO and control ischemic mice exhibited

Figure 1. Infarct Area and Mortality Rate Are Increased in stVAChT-KO Mice After Ischemia-Reperfusion. (a) Representative T_2-weighted magnetic resonance images and TCC stained coronal sections from wild-type mice that had MCAO for 30, 45 and 60 min as well as 24 hr. Images were obtained 24 hr after MCAO. (b) Quantitative analysis of experiments performed in A. (c) Representative T_2-weighted magnetic resonance images of coronal sections from stVAChT-KO mice and littermate controls obtained 24 hr after mice were submitted to 60 min MCAO. (d) Quantitative analysis of experiments performed in C. (e) Survival curves estimated using Kaplan–Meier test. TTC = triphenyltetrazolium chloride; MRI = magnetic resonance imaging; stVAChT-KO = selective vesicular acetylcholine transporter-deficient mice; CTR = control.

Table 1. Physiological Parameters Measured 24 hr Following Ischemic Insult.

Physiological parameters	Control	stVAChT-KO	Unpaired t test (p value)
Before MCAO			
Heart rate, beats/min	732.4 ± 23.44	712.6 ± 46.00	.7114
During MCAO			
Heart rate, beats/min	724.6 ± 38.98	658.4 ± 36.47	.2501
24 hr after MCAO			
Heart rate, beats/min	682.2 ± 67.23	663.6 ± 35.33	.8127
Arterial blood pH	7.208 ± 0.0361	7.206 ± 0.0249	.9612
Oxygen saturation, %	96.32 ± 3.952	98.38 ± 3.682	.7129
Temperature, °C	35.56 ± 0.2502	35.44 ± 0.4167	.8112
Glucose	3.320 ± 0.5444	3.320 ± 0.3426	1
pO_2	156.2 ± 43.18	184.1 ± 47.67	.6755
pCO_2	38.06 ± 4.674	36.34 ± 1.580	.7364

Note. MCAO = middle cerebral artery occlusion; stVAChT-KO = selective vesicular acetylcholine transporter-deficient mice.
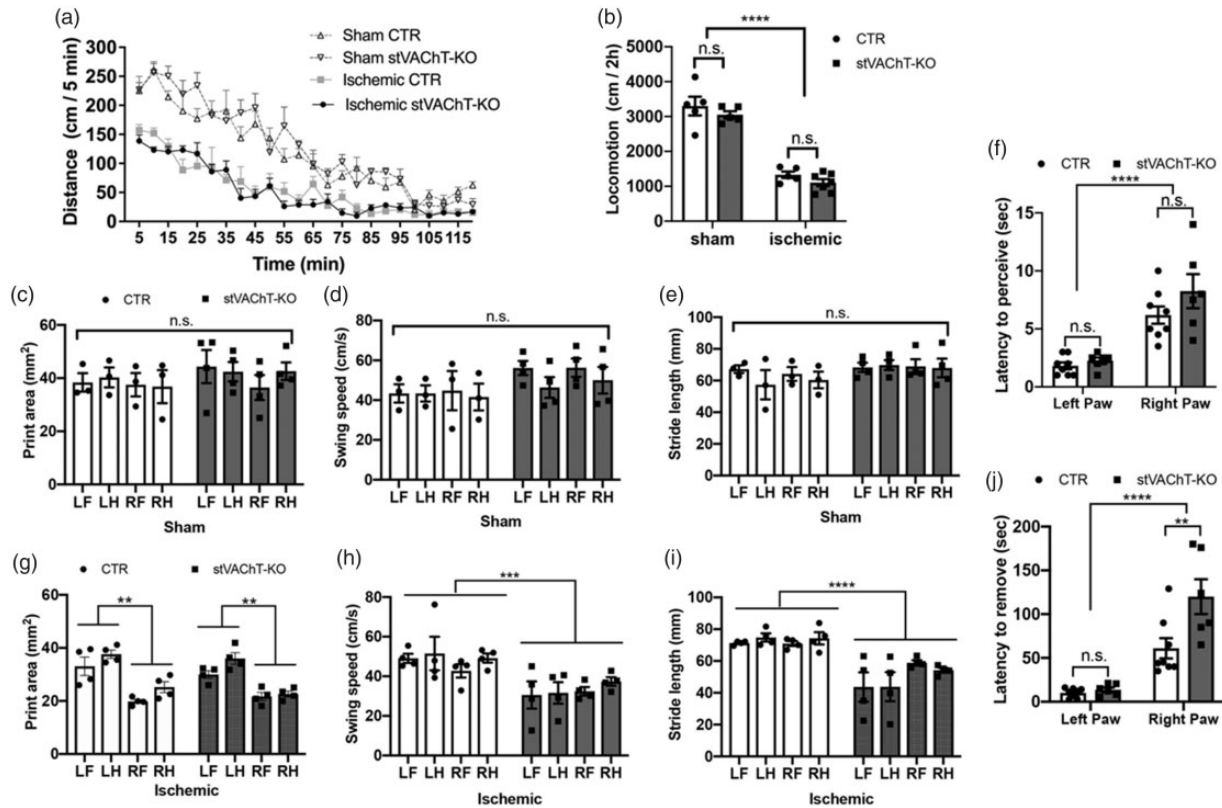
Figure 2. Gait and Sensorimotor Deficits Are More Pronounced in stVAChT-KO Mice After Ischemia-Reperfusion. (a) Horizontal locomotor activity in an open-field for stVAChTD2-KO and littermate control mice measured in bouts of 5 min. (b) Cumulative 2 hr locomotion for stVAChTD2-KO and littermate controls. (c–h). Analysis of gait in the CatWalk test in sham (c–e) and MCAO (f–h) stVAChT-KO and littermate controls. Print area (c and f); Swing speed (d and g); Stride length (e and h). (i) Latency to perceive adhesive tape stuck into each forelimb. (j) Latency to remove adhesive tape stuck into each forelimb. Asterisks indicate significant effect of genotype by two-way Anova. **$p < .01$. ***$p < .001$; $p < .0001$, n.s. = nonsignificant; stVAChT-KO = selective vesicular acetylcholine transporter-deficient mice; CTR = control. Data are shown as mean (+ SEM). White columns: controls, Gray columns: stVAChT-KO.

significantly reduced total locomotor activity (Figure 2A and B) when compared with sham-operated mice (two-way ANOVA; main effect of treatment $F(1, 18) = 165.8$, $p < .0001$). However, there was no difference in locomotor behavior between genotypes (two-way ANOVA; no effect of genotype; $F(1, 18) = 2.452$, $p = .1348$).

To evaluate whether ischemic injury affected mobility, we investigated gait parameters using an automated CatWalk system. Sham-operated stVAChT-KO and littermate controls were able to easily traverse the walkway and no difference between the two groups was observed on all the parameters measured, including print area, swing speed and stride length (Figure 2C to E). Also, parameters observed on sham-operated stVAChT-KO and littermate controls are compatible with data in the literature for nonoperated wild-type mice (Caballero-Garrido et al., 2017; Janickova et al., 2017b). These results indicate that gait parameters are similar in both stVAChT-KO and littermate controls and that these parameters were not affected by the surgery. On the

other hand, ischemic stVAChT-KO and littermate controls displayed clear gait alterations (Figure 2F to H). Both genotypes showed a similar decrease in print area on the affected side—Figure 2F; two-way ANOVA; main effect on paws; $F(3, 24) = 28.52$, $p < .0001$; no effect of genotype; $F(1, 24) = 0.97$, $p = .33$. In addition, stVAChT-KO exhibited a slower swing speed (Figure 2G) and shorter stride lengths (Figure 2H), when compared to ischemic control mice—two-way ANOVA; main effect genotype; $F(1, 24) = 20.49$, $p = .0001$. These results indicate that the effect of ischemia on gait function is significantly more pronounced in mice with decreased striatum ACh than in littermate controls.

We also evaluated fine sensorimotor function on ischemic stVAChT-KO and littermate controls using the adhesive removal test. Both genotypes showed increased latency to perceive the tape on the contralateral paw (right paw, Figure 2I) compared to the ipsilateral paw—two-way ANOVA; main effect of paw side; $F(1, 24) = 42.92$, $p < .0001$, but there was no difference
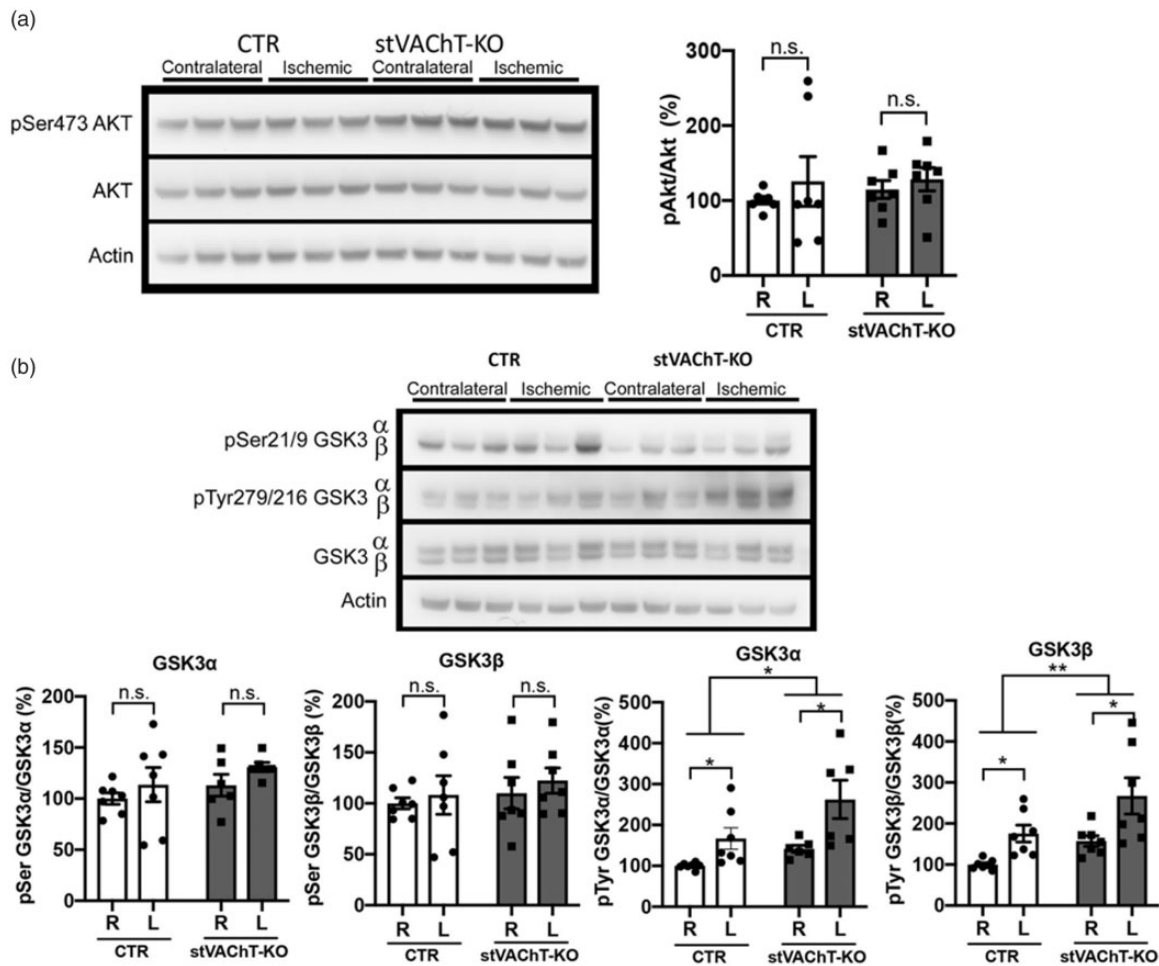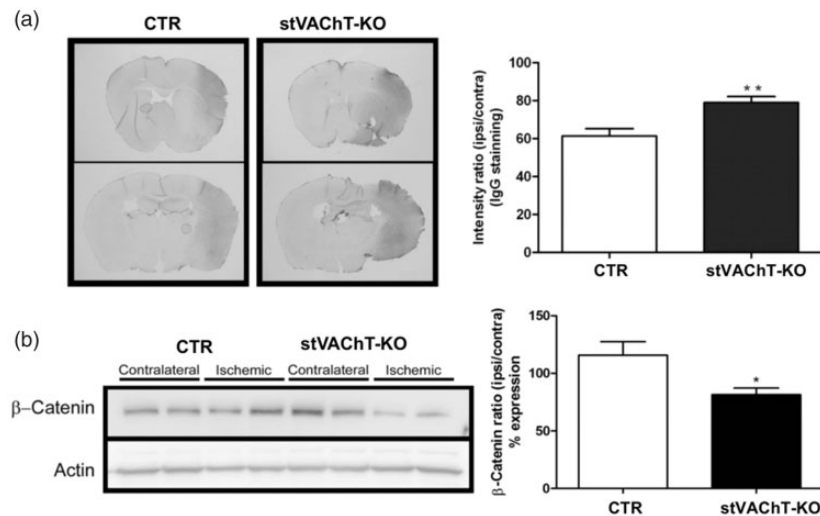
Figure 3. stVAChT-KO Mice Show a Higher Increase in Activated GSK3-β After Ischemia-Reperfusion. (a) Representative immunoblot (left) and quantitative analysis (right) of pSer473 AKT, total AKT and actin in the striatal tissue of stVAChTD2-KO and controls. (b) Representative immunoblot (top) and quantitative analysis (bottom) of pSer 21/9 GSK3α and GSK3β; pTyr 279/216 GSK3α and GSK3β, total GSK3α and GSK3β and actin in the striatal tissue of stVAChTD2-KO and controls. Protein levels were normalized using actin. n.s. = nonsignificant; stVAChT-KO = selective vesicular acetylcholine transporter-deficient mice; CTR = control. $*p < .05$. $**p < .01$.

between genotypes—two-way ANOVA; no effect of genotype; $F(1, 24) = 2.492$, $p = .127$. Likewise, both stVAChT-KO and littermate controls took longer to remove the tape from the contralateral side (right side) than from the ipsilateral side—Figure 2J; two-way ANOVA; main effect of paw side; $F(1, 24) = 51.21$, $p < .0001$. However, stVAChT-KO took longer than littermate controls to remove the tape from the contralateral side—main effect of genotype; $F(1, 24) = 8.12$, $p = .0088$; Turkey's multiple comparisons test: Right Paw:CTR vs. Right Paw:stVAChT-KO adj $p = .0046$. No genotype difference was observed on the time to remove the tape from the ipsilateral side (Turkey's multiple comparisons test: Left Paw:CTR vs. Left Paw: stVAChT-KO adj $p = .995$). Taken together, these results indicate ischemia leads to a larger sensorimotor impairment in stVAChT-KO mice than on littermate controls.

stVAChT-KO Mice Show a Higher Increase in Activated GSK3-β After Ischemia-Reperfusion

Recent studies show that α7nAChR stimulation modulates PI3K/Akt signalling which in turn reduces activated GSK-3β, leading to improved functional and morphological outcomes after cerebral injuries in rodents (Krafft et al., 2012, 2013; Y. Sun et al., 2017). Conversely, decreased cholinergic signaling in the hippocampus has been demonstrated to influence the PI3K/Akt signaling pathway leading to increased levels of activated GSK-3β and associated increased neuronal death (Kolisnyk et al., 2017). To determine whether reduced levels of striatal ACh affect PI3K/Akt-GSK-3 signaling after stroke injury, we performed immunoblot analyses on striatum samples collected 24 hr after MCAO and quantified changes in levels of pAkt (Ser473) as a ratio of total Akt (Figure 3A). No differences in p-Akt levels were

Figure 4. stVAChT-KO Mice Show Higher Increase in Blood–Brain Barrier Permeability After Ischemia-Reperfusion. (a) Representative coronal sections stained with goat anti-mouse IgG conjugated with HRP and quantitative analysis. (b) Representative immunoblot and quantitative analysis of β-catenin GSK3β and actin in the striatal tissue of stVAChTD2-KO and controls. stVAChT-KO = selective vesicular acetylcholine transporter-deficient mice; CTR = control. *$p < .05$. **$p < .01$.

observed between ipsilateral and contralateral striatal brain hemispheres or between genotypes—two-way ANOVA; no effect of brain hemisphere; $F(1, 12) = 1.212$, $p = .293$; no effect of genotype; $F(1, 12) = 0.177$, $p = .682$; no interaction: $F(1, 12) = 0.110$, $p = .746$.

Several proapoptotic stimuli, including oxygen glucose deprivation, have been reported to increase GSK-3β activity, which is related to an increase in Tyr216 phosphorylation (Bhat et al., 2000). Conversely, inhibition of GSK-3β, correlated to increased phosphorylation of Ser9, is associated with activation of neuronal survival pathways (Garcia-Segura et al., 2007). We measured Ser9 phosphorylation levels of GSK-3α and GSK-3β in the striatum of stVAChT-KO and littermate controls but did not find any difference (Figure 3B). Specifically, p-GSK-3α/β(Ser21/Ser9) levels were not different between brain hemispheres or genotypes—two-way ANOVA, p-GSK-3α(Ser21): no effect of brain hemisphere; $F(1, 24) = 3.270$, $p = .083$; no interaction of genotype; $F(1, 24) = 3.337$, $p = .080$; no interaction: $F(1, 24) = 0.375$, $p = .546$; p-GSK3β(Ser9): no effect of brain hemisphere; $F(1, 24) = 0.542$, $p = .468$; no effect of genotype; $F(1, 24) = 0.750$, $p = .395$; no interaction: $F(1, 24) = 0.023$, $p = .881$. On the other hand, GSK3 (Tyr279/Tyr216) phosphorylation differed between hemispheres and between genotypes (Figure 3B). That is, in both genotypes p-GSK-3α(Tyr279) and p-GSK-3β(Tyr216) were increased in the left hemisphere (ischemic) when compared to the right (contralateral) side—two-way ANOVA; p-GSK-3α(Tyr279): main effect of brain hemisphere; $F(1, 24) = 10.43$, $p = .004$; p-GSK3β (Tyr216: main effect of hemisphere $F(1, 24) = 13.46$, $p = .0012$—and the effect was more prominent on stVAChT-KO

when compared to littermate controls—two-way ANOVA; p-GSK3α(Tyr279): main effect genotype; $F(1, 24) = 4.78$, $p = .039$; p-GSK3β(Tyr216): main effect of genotype, $F(1, 24) = 8.698$, $p = .007$. These results suggest that GSK-3 activation is increased after ischemic stroke and that this effect is more pronounced in stVAChT-KO mice compared to controls.

GSK-3 is essential for the control of cellular levels of β-catenin (C. Liu et al., 2002), a cell adhesion protein that plays important roles in BBB formation, maturation, and integrity (Liebner et al., 2008; Tran et al., 2016). Given the increase in p-GSK-3 suggests increased activation, we tested whether β-catenin levels and BBB permeability could be affected in mice with decreased striatal VAChT levels when compared to control mice. The results showed reduced levels of β-catenin in stVAChT-KO mice compared to control mice after MCAO (Student's t test; $t(14) = 2.624$, $p = .02$, Figure 4B). To investigate BBB integrity, we used immunohistochemistry to examine extravascular IgG staining in the brain parenchyma. Our results showed increased intensity of IgG staining in stVAChT-KO mouse brains compared to control mice (Student's t test; $t(22) = 3.509$, $p = .002$; Figure 4A). These results suggest that the BBB is more permeable in stVAChT-KO mice compared to controls, likely contributing to the worse outcomes observed in these mutant mice.

Discussion

In this study, we investigated the role of endogenous striatal cholinergic activity on injury and recovery after an ischemic insult. Our results demonstrate that an

ischemic insult in mice with decreased ACh release in the striatum results in larger infarct size, more pronounced functional impairments and increased mortality than in littermate controls. In addition, our data suggest that these detrimental effects might be related to increased activation of GSK-3 and a higher permeability of the BBB. It should be noted that because we used mice that present deficits in cholinergic signaling from early age, it is possible that some of the phenotypes described may be influenced by loss of cholinergic signaling during development.

Interestingly, recent imaging studies in humans suggest a protective role of ACh against cerebral ischemia. Patients with cholinergic lesions (assessed by MRI) were shown to have poor functional outcome after stroke (Qu et al., 2018). In addition, pharmacological upregulation of cholinergic activity by administration of different cholinesterase inhibitors shortly after acute ischemic stroke has been shown to result in reduced lesion volumes and improved functional recovery (Z. F. Wang, Wang, et al., 2008; Barrett et al., 2011; Zhao et al., 2011; Chang et al., 2017). Similar neuroprotective effects have also been observed upon administration of nicotinic agonists (Chen et al., 2017) or positive allosteric alpha7 nicotinic modulators (Gaidhani & Uteshev, 2018).

Gait dysfunction following stroke is highly prevalent in humans (Handlery et al., 2020; Little et al., 2020) and is also observed after different models of stroke in rodents (Y. Wang, Bontempi, et al., 2008; Y. Liu et al., 2013; Fluri et al., 2017). Thus, we used gait analysis as one of the parameters to compare functional deficits in stVAChT-KO mice and littermate controls 7 days after stroke. Our results showed that, although both genotypes decreased the use of the paws plantar surface on the affected side, stVAChT-KO mice—but not littermate controls—also exhibited shorter and slower steps on the affected side. To note, shorter and slower steps are characteristics observed in humans after stroke (Handlery et al., 2020) as well as in Parkinson's patients (Knutsson, 1972) and rodent models of Parkinson's disease (Vlamings et al., 2007). Strikingly, mice with mesopontine cholinergic deficiency, a dysfunction commonly seen in Parkinson's disease, also show decreased use of paws plantar surface as well as short and slower steps (Janickova et al., 2017b). Thus, it is possible that both increased lesion size and decreased cholinergic signaling contribute to the worse gait deficiencies observed in stVAChT-KO mice. It should be noted that in our experimental design, we did not test mice in other time points for gait, which is a limitation of this study.

Activation of alpha 7 nicotinic ACh receptors has been shown to improve functional recovery for cerebral injuries through activation of Akt and subsequent inactivation of GSK3β (Duris et al., 2011; Krafft et al., 2012; Y. Sun et al., 2017). Akt is a Ser/Thr kinase that is directly activated by PI3K-mediated phosphorylation (Manning & Toker, 2017). Activated Akt (p-Akt) is able to inhibit GSK3β, by phosphorylation of Ser 9. GSK3 has two isoforms, GSK3α and GSK3β, which are functionally redundant in some contexts, but also show some isoform-specific functions (Hoffmeister et al., 2020). Our results showed that activated p-Akt levels and correlated levels of p-GSK3β(Ser9)/p-GSK3α (Ser21) were unchanged when the injured side was compared to the uninjured side, both in stVAChT-KO mice and littermate controls. Levels of activated p-GSK3α (Tyr279) and p-GSK3β(Tyr216) were increased in the ischemic hemisphere when compared to uninjured side of both stVAChT-KO mice and littermate controls. However, phosphorylation was more prominent on stVAChT-KO when compared to littermate controls. These results suggest that, similar to data reported for the hippocampus (Kolisnyk et al., 2017), decreased cholinergic signaling in the striatum leads to increased levels of activated GSK-3 and support a neuroprotective role for striatum cholinergic signaling.

Increase of p-GSK3β(Tyr216) has been suggested to represent an important mechanism by which cellular insults induced by ischemia can lead to neuronal death (Bhat et al., 2000; D'Angelo et al., 2016). Conversely, GSK-3β inhibition has been shown to protect the BBB and attenuate early ischemia-reperfusion stroke injury, possibly by early activation of the Wnt/β-catenin signaling pathway (W. Wang et al., 2017; Jean LeBlanc et al., 2019). Brain edema, the accumulation of fluid within the brain tissue, is a critical consequence of ischemia-reperfusion (Y. Yang & Rosenberg, 2011; Thrane et al., 2014). Early during ischemia-reperfusion (<24 hr), edema results mainly from cytotoxic and ionic insults, while blood vessel damage with breakdown of the BBB is relevant for delayed (24–72 hr) cerebral edema (Y. Yang & Rosenberg, 2011; Thrane et al., 2014). Recent pharmacological studies suggest that cholinergic receptor activation on epithelial/endothelial cells regulates the expression of tight junction proteins, such as occludin, claudins, and junctional adhesion molecule-1, which are present at the membrane of two adjacent endothelial cells and are essential constituents of the BBB (Krafft et al., 2013; Dhawan et al., 2015; Tang et al., 2017; N. Y. Yang et al., 2017; Zou et al., 2017; Kimura et al., 2019). Our data suggest that cholinergic signaling can also influence β-catenin levels. β-catenin, a component of adhesion junctions, plays an essential role in the regulation and coordination of cell–cell adhesion and can also shuttle from the membrane to the nucleus where it functions as a co-transcription factor in the canonical Wnt signaling pathway (Brembeck et al., 2006; MacDonald et al., 2009). Specifically, β-catenin connects VE-cadherin to the actin cytoskeleton stabilizing adherens junctions and controlling vascular permeability and integrity

(Dejana et al., 2009). Under normal conditions, canonical Wnt signaling increases cytoplasmic accumulation of β-catenin by blocking its phosphorylation by GSK3β (MacDonald et al., 2009). Stabilized β-catenin translocates to the nucleus, where it activates expression of several genes involved in cell proliferation, survival, differentiation, neurogenesis, inflammation, as well as BBB formation and function (Libro et al., 2016; Ziegler et al., 2016). Different stimuli including ischemia events activate the ubiquitously expressed GSK3-β, which phosphorylates β-catenin on several serine/threonine residues leading to ubiquitin-mediated proteosomal degradation of β-catenin (Rubinfeld et al., 1996). Together, these results suggest that decreased levels of β-catenin observed in the ischemic side of stVAChT-KO mice brain might contribute for both, the deficit in BBB integrity and the larger infarct size. Additional studies are warranted to investigate whether the expression level of tight junction proteins, such as claudins and ocludins, are altered in stVAChT-KO mice after ischemia.

In short, mice with decreased ACh signaling in the striatum showed worse outcome after ischemia-reperfusion, including larger infarct size, more pronounced functional impairments and increased mortality. These changes were paralleled by increased activation of GSK-3, decreased levels of β-catenin and destabilization of the BBB. These results support a protective role for ACh against cerebral ischemia and suggest that pro-cholinergic drugs have potential therapeutic benefits in the amelioration of BBB permeability.

Acknowledgment

Author Contributions

D. F. G., M. S. G., S. R., and R. G. performed experiments and analyzed data. A. R. M., R. G., R. B., V. F. P., and M. A. M. P. acquired funding and provided guidance. D. F. G., M. S. G., V. F. P., R. B., and M. A. M. P. wrote manuscript. All authors edited and agreed with the last version of the manuscript. D. F. G. and M. S. G. contributed equally to this work.

Declaration of Conflicting Interests

The author(s) declared no potential conflicts of interest with respect to the research, authorship, and/or publication of this article.

Ethics Approval

Animal protocol numbers approved by The University of Western Ontario (2016-104). This study followed the ARRIVE guidelines.

Funding

ORCID iDs

Vania F. Prado (ID) https://orcid.org/0000-0003-4994-6393
Marco A. M. Prado (ID) https://orcid.org/0000-0002-3028-5778

Summary Statement

Cholinergic tone regulates blood–brain barrier permeability and recovery after stroke.

References

Andsberg, G., Kokaia, Z., & Lindvall, O. (2001). Upregulation of p75 neurotrophin receptor after stroke in mice does not contribute to differential vulnerability of striatal neurons. *Exp Neurol*, *169*(2), 351–363.

Barrett, K. M., Brott, T. G., Brown, R. D., Jr., Carter, R. E., Geske, J. R., Graff-Radford, N. R., McNeil, R. B., & Meschia, J. F. (2011). Enhancing recovery after acute ischemic stroke with donepezil as an adjuvant therapy to standard medical care: Results of a phase IIA clinical trial. *J Stroke Cerebrovasc Dis*, *20*(3), 177–182.

Bederson, J. B., Pitts, L. H., Tsuji, M., Nishimura, M. C., Davis, R. L., & Bartkowski, H. (1986). Rat middle cerebral artery occlusion: Evaluation of the model and development of a neurologic examination. *Stroke*, *17*(3), 472–476.

Belayev, L., Busto, R., Zhao, W., Fernandez, G., & Ginsberg, M. D. (1999). Middle cerebral artery occlusion in the mouse by intraluminal suture coated with poly-L-lysine: Neurological and histological validation. *Brain Res*, *833*(2), 181–190.

Benedek, A., Moricz, K., Juranyi, Z., Gigler, G., Levay, G., Harsing, L. G., Jr., Matyus, P., Szenasi, G., & Albert, M. (2006). Use of TTC staining for the evaluation of tissue injury in the early phases of reperfusion after focal cerebral ischemia in rats. *Brain Res*, *1116*(1), 159–165.

Beraldo, F. H., et al. (2013). Stress-inducible phosphoprotein 1 has unique cochaperone activity during development and regulates cellular response to ischemia via the prion protein. *FASEB J*, *27*(9), 3594–3607.

Bhat, R. V., Shanley, J., Correll, M. P., Fieles, W. E., Keith, R. A., Scott, C. W., & Lee, C. M. (2000). Regulation and localization of tyrosine216 phosphorylation of glycogen synthase kinase-3beta in cellular and animal models of neuronal degeneration. *Proc Natl Acad Sci U S A*, *97*(20), 11074–11079.

Bouet, V., Boulouard, M., Toutain, J., Divoux, D., Bernaudin, M., Schumann-Bard, P., & Freret, T. (2009). The adhesive removal test: A sensitive method to assess sensorimotor deficits in mice. *Nat Protoc*, *4*(10), 1560–1564.

Brembeck, F. H., Rosario, M., & Birchmeier, W. (2006). Balancing cell adhesion and wnt signaling, the key role of beta-catenin. *Curr Opin Genet Dev*, *16*(1), 51–59.

Caballero-Garrido, E., Pena-Philippides, J. C., Galochkina, Z., Erhardt, E., & Roitbak, T. (2017). Characterization of long-term gait deficits in mouse dMCAO, using the CatWalk system. *Behav Brain Res*, 331, 282–296.

Chang, C. F., Lai, J. H., Wu, J. C., Greig, N. H., Becker, R. E., Luo, Y., Chen, Y. H., Kang, S. J., Chiang, Y. H., & Chen, K. Y. (2017). (-)-phenserine inhibits neuronal apoptosis following ischemia/reperfusion injury. *Brain Res*, 1677, 118–128.

Chen, S., Bennet, L., & McGregor, A. L. (2017). Delayed varenicline administration reduces inflammation and improves forelimb use following experimental stroke. *J Stroke Cerebrovasc Dis*, 26(12), 2778–2787.

Conner, J. M., Chiba, A. A., & Tuszynski, M. H. (2005). The basal forebrain cholinergic system is essential for cortical plasticity and functional recovery following brain injury. *Neuron*, 46(2), 173–179.

Conner, J. M., Culberson, A., Packowski, C., Chiba, A. A., & Tuszynski, M. H. (2003). Lesions of the basal forebrain cholinergic system impair task acquisition and abolish cortical plasticity associated with motor skill learning. *Neuron*, 38(5), 819–829.

D'Angelo, B., Ek, C. J., Sun, Y., Zhu, C., Sandberg, M., & Mallard, C. (2016). GSK3beta inhibition protects the immature brain from hypoxic-ischaemic insult via reduced STAT3 signalling. *Neuropharmacology*, 101, 13–23.

de Castro, B. M., De Jaeger, X., Martins-Silva, C., Lima, R. D. F., Amaral, E., Menezes, C., Lima, P., Neves, C. M. L., Pires, R. G., Gould, T. W., Welch, I., Kushmerick, C., Guatimosim, C., Izquierdo, I., Cammarota, M., Rylett, R. J., Gomez, M. V., Caron, M. G., Oppenheim, R. W., Prado, M. A. M., & Prado, V. F. (2009). The vesicular acetylcholine transporter is required for neuromuscular development and function. *Mol Cell Biol*, 29(19), 5238–5250.

de Castro, B. M., Pereira, G. S., Magalhaes, V., Rossato, J. I., De Jaeger, X., Martins-Silva, C., Leles, B., Lima, P., Gomez, M. V., Gainetdinov, R. R., Caron, M. G., Izquierdo, I., Cammarota, M., Prado, V. F., & Prado, M. A. (2009). Reduced expression of the vesicular acetylcholine transporter causes learning deficits in mice. *Genes Brain Behavior*, 8(1), 23–35.

Dejana, E., Tournier-Lasserve, E., & Weinstein, B. M. (2009). The control of vascular integrity by endothelial cell junctions: Molecular basis and pathological implications. *Dev Cell*, 16(2), 209–221.

Deng, P., Zhang, Y., & Xu, Z. C. (2008). Inhibition of Ih in striatal cholinergic interneurons early after transient forebrain ischemia. *J Cereb Blood Flow Metab*, 28(5), 939–947.

Dhawan, S., Hiemstra, I. H., Verseijden, C., Hilbers, F. W., Te Velde, A. A., Willemsen, L. E., Stap, J., den Haan, J. M., & de Jonge, W. J. (2015). Cholinergic receptor activation on epithelia protects against cytokine-induced barrier dysfunction. *Acta Physiol*, 213(4), 846–859.

Duris, K., Manaenko, A., Suzuki, H., Rolland, W. B., Krafft, P. R., & Zhang, J. H. (2011). α7 nicotinic acetylcholine receptor agonist PNU-282987 attenuates early brain injury in a perforation model of subarachnoid hemorrhage in rats. *Stroke*, 42(12), 3530–3536.

Fluri, F., Malzahn, U., Homola, G. A., Schuhmann, M. K., Kleinschnitz, C., & Volkmann, J. (2017). Stimulation of the mesencephalic locomotor region for gait recovery after stroke. *Ann Neurol*, 82(5), 828–840.

Gaidhani, N., & Uteshev, V. V. (2018). Treatment duration affects cytoprotective efficacy of positive allosteric modulation of alpha7 nAChRs after focal ischemia in rats. *Pharmacol Res*, 136, 121–132.

Garcia-Segura, L. M., Diz-Chaves, Y., Perez-Martin, M., & Darnaudery, M. (2007). Estradiol, insulin-like growth factor-I and brain aging. *Psychoneuroendocrinology*, 32 Suppl 1, S57–S61.

Guzman, M. S., De Jaeger, X., Raulic, S., Souza, I. A., Li, A. X., Schmid, S., Menon, R. S., Gainetdinov, R. R., Caron, M. G., Bartha, R., Prado, V. F., & Prado, M. A. (2011). Elimination of the vesicular acetylcholine transporter in the striatum reveals regulation of behaviour by cholinergic-glutamatergic co-transmission. *PLoS Biol*, 9(11), e1001194.

Handlery, R., Fulk, G., Pellegrini, C., Stewart, J. C., Monroe, C., & Fritz, S. (2020). Stepping after stroke: Walking characteristics in people with chronic stroke differ on the basis of walking speed, walking endurance, and daily steps. *Phys Ther*, 100(5), 807–817.

Hoffmeister, L., Diekmann, M., Brand, K., & Huber, R. (2020). GSK3: A kinase balancing promotion and resolution of inflammation. *Cells*, 9(4), 820.

Janickova, H., Prado, V. F., Prado, M. A. M., El Mestikawy, S., & Bernard, V. (2017a). Vesicular acetylcholine transporter (VAChT) over-expression induces major modifications of striatal cholinergic interneuron morphology and function. *J Neurochem*, 142(6), 857–875.

Janickova, H., Rosborough, K., Al-Onaizi, M., Kljakic, O., Guzman, M. S., Gros, R., Prado, M. A., & Prado, V. F. (2017b). Deletion of the vesicular acetylcholine transporter from pedunculopontine/laterodorsal tegmental neurons modifies gait. *J Neurochem*, 140(5), 787–798.

Jean LeBlanc, N., Menet, R., Picard, K., Parent, G., Tremblay, M. E., & ElAli, A. (2019). Canonical wnt pathway maintains blood-brain barrier integrity upon ischemic stroke and its activation ameliorates tissue plasminogen activator therapy. *Mol Neurobiol*, 56(9), 6521–6538.

Katchanov, J., Waeber, C., Gertz, K., Gietz, A., Winter, B., Bruck, W., Dirnagl, U., Veh, R. W., & Endres, M. (2003). Selective neuronal vulnerability following mild focal brain ischemia in the mouse. *Brain Pathol*, 13(4), 452–464.

Kawaguchi, Y., Wilson, C. J., Augood, S. J., & Emson, P. C. (1995). Striatal interneurones: Chemical, physiological and morphological characterization. *Trends Neurosci*, 18(12), 527–535.

Kimura, I., Dohgu, S., Takata, F., Matsumoto, J., Kawahara, Y., Nishihira, M., Sakada, S., Saisho, T., Yamauchi, A., & Kataoka, Y. (2019). Activation of the alpha7 nicotinic acetylcholine receptor upregulates blood-brain barrier function through increased claudin-5 and occludin expression in rat brain endothelial cells. *Neurosci Lett*, 694, 9–13.

Kljakic, O., Janickova, H., Prado, V. F., & Prado, M. A. M. (2017). Cholinergic/glutamatergic co-transmission in striatal cholinergic interneurons: New mechanisms regulating

striatal computation. *J Neurochem*, *142 Suppl 2*(Suppl 2), 90–102.

Knutsson, E. (1972). An analysis of Parkinsonian gait. *Brain*, *95*(3), 475–486.

Kolisnyk, B., Al-Onaizi, M. A., Hirata, P. H., Guzman, M. S., Nikolova, S., Barbash, S., Soreq, H., Bartha, R., Prado, M. A., & Prado, V. F. (2013b). Forebrain deletion of the vesicular acetylcholine transporter results in deficits in executive function, metabolic, and RNA splicing abnormalities in the prefrontal cortex. *J Neurosci*, *33*(37), 14908–14920.

Kolisnyk, B., Al-Onaizi, M., Soreq, L., Barbash, S., Bekenstein, U., Haberman, N., Hanin, G., Kish, M. T., da Silva, J. S., Fahnestock, M., Ule, J., Soreq, H., Prado, V. F., & Prado, M. A. M. (2017). Cholinergic surveillance over hippocampal RNA metabolism and Alzheimer's-like pathology. *Cereb Cortex*, *27*, 3553–3567.

Kolisnyk, B., Guzman, M. S., Raulic, S., Fan, J., Magalhaes, A. C., Feng, G. P., Gros, R., Prado, V. F., & Prado, M. A. M. (2013a). ChAT-ChR2-EYFP mice have enhanced motor endurance but show deficits in attention and several additional cognitive domains. *J Neurosci*, *33*(25), 10427–10438.

Krafft, P. R., Altay, O., Rolland, W. B., Duris, K., Lekic, T., Tang, J., & Zhang, J. H. (2012). α7 nicotinic acetylcholine receptor agonism confers neuroprotection through GSK-3beta inhibition in a mouse model of intracerebral hemorrhage. *Stroke*, *43*(3), 844–850.

Krafft, P. R., Caner, B., Klebe, D., Rolland, W. B., Tang, J., & Zhang, J. H. (2013). PHA-543613 preserves blood-brain barrier integrity after intracerebral hemorrhage in mice. *Stroke*, *44*(6), 1743–1747.

Libro, R., Bramanti, P., & Mazzon, E. (2016). The role of the wnt canonical signaling in neurodegenerative diseases. *Life Sci*, *158*, 78–88.

Liebner, S., Corada, M., Bangsow, T., Babbage, J., Taddei, A., Czupalla, C. J., Reis, M., Felici, A., Wolburg, H., Fruttiger, M., Taketo, M. M., von Melchner, H., Plate, K. H., Gerhardt, H., & Dejana, E. (2008). Wnt/beta-catenin signaling controls development of the blood-brain barrier. *J Cell Biol*, *183*(3), 409–417.

Lima, R. D. F., Prado, V. F., Prado, M. A. M., & Kushmerick, C. (2010). Quantal release of acetylcholine in mice with reduced levels of the vesicular acetylcholine transporter. *J Neurochem*, *113*(4), 943–951.

Little, V. L., Perry, L. A., Mercado, M. W. V., Kautz, S. A., & Patten, C. (2020). Gait asymmetry pattern following stroke determines acute response to locomotor task. *Gait Posture*, *77*, 300–307.

Liu, C., Li, Y., Semenov, M., Han, C., Baeg, G. H., Tan, Y., Zhang, Z., Lin, X., & He, X. (2002). Control of beta-catenin phosphorylation/degradation by a dual-kinase mechanism. *Cell*, *108*(6), 837–847.

Liu, Y., Ao, L. J., Lu, G., Leong, E., Liu, Q., Wang, X. H., Zhu, X. L., Sun, T. F., Fei, Z., Jiu, T., Hu, X., & Poon, W. S. (2013). Quantitative gait analysis of long-term locomotion deficits in classical unilateral striatal intracerebral hemorrhage rat model. *Behav Brain Res*, *257*, 166–177.

Longa, E. Z., Weinstein, P. R., Carlson, S., & Cummins, R. (1989). Reversible middle cerebral artery occlusion without craniectomy in rats. *Stroke*, *20*(1), 84–91.

Lorrio, S., Sobrado, M., Arias, E., Roda, J. M., Garcia, A. G., & Lopez, M. G. (2007). Galantamine postischemia provides neuroprotection and memory recovery against transient global cerebral ischemia in gerbils. *J Pharmacol Exp Ther*, *322*(2), 591–599.

MacDonald, B. T., Tamai, K., & He, X. (2009). Wnt/beta-catenin signaling: Components, mechanisms, and diseases. *Dev Cell*, *17*(1), 9–26.

Manning, B. D., & Toker, A. (2017). AKT/PKB signaling: Navigating the network. *Cell*, *169*(3), 381–405.

Martyn, A. C., De Jaeger, X., Magalhaes, A. C., Kesarwani, R., Goncalves, D. F., Raulic, S., Guzman, M. S., Jackson, M. F., Izquierdo, I., Macdonald, J. F., Prado, M. A., & Prado, V. F. (2012). Elimination of the vesicular acetylcholine transporter in the forebrain causes hyperactivity and deficits in spatial memory and long-term potentiation. *Proc Natl Acad Sci U S A*, *109*(43), 17651–17656.

McVicar, N., Li, A. X., Goncalves, D. F., Bellyou, M., Meakin, S. O., Prado, M. A., & Bartha, R. (2014). Quantitative tissue pH measurement during cerebral ischemia using amine and amide concentration-independent detection (AACID) with MRI. *J Cereb Blood Flow Metab*, *34*(4), 690–698.

Pham, M., Helluy, X., Kleinschnitz, C., Kraft, P., Bartsch, A. J., Jakob, P., Nieswandt, B., Bendszus, M., & Stoll, G. (2011). Sustained reperfusion after blockade of glycoprotein-receptor-Ib in focal cerebral ischemia: An MRI study at 17.6 tesla. *PLoS One*, *6*(4), e18386.

Prado, V. F., Janickova, H., Al-Onaizi, M. A., & Prado, M. A. (2017). Cholinergic circuits in cognitive flexibility. *Neuroscience*, *345*, 130–141.

Prado, V. F., et al. (2006). Mice deficient for the vesicular acetylcholine transporter are myasthenic and have deficits in object and social recognition. *Neuron*, *51*(5), 601–612.

Prado, V. F., Roy, A., Kolisnyk, B., Gros, R., & Prado, M. A. (2013). Regulation of cholinergic activity by the vesicular acetylcholine transporter. *Biochem J*, *450*(2), 265–274.

Qu, J. F., Chen, Y. K., Luo, G. P., Zhao, J. H., Zhong, H. H., & Yin, H. P. (2018). Severe lesions involving cortical cholinergic pathways predict poorer functional outcome in acute ischemic stroke. *Stroke*, *49*(12), 2983–2989.

Rubinfeld, B., Albert, I., Porfiri, E., Fiol, C., Munemitsu, S., & Polakis, P. (1996). Binding of GSK3beta to the APC-beta-catenin complex and regulation of complex assembly. *Science*, *272*(5264), 1023–1026.

Sakae, D. Y., et al. (2015). The absence of VGLUT3 predisposes to cocaine abuse by increasing dopamine and glutamate signaling in the nucleus accumbens. *Mol Psychiatry*, *20*(11), 1448–1459.

Sugita, S., Fleming, L. L., Wood, C., Vaughan, S. K., Gomes, M., Camargo, W., Naves, L. A., Prado, V. F., Prado, M. A. M., Guatimosim, C., & Valdez, G. (2016). VAChT overexpression increases acetylcholine at the synaptic cleft and accelerates aging of neuromuscular junctions. *Skelet Muscle*, *6*(1), 31.

Sun, B., Chen, L., Wei, X., Xiang, Y., Liu, X., & Zhang, X. (2011). The akt/GSK-3beta pathway mediates flurbiprofen-induced neuroprotection against focal cerebral ischemia/reperfusion injury in rats. *Biochem Biophys Res Commun*, *409*(4), 808–813.

Sun, Y., Song, D., Wang, M., Chen, K., & Zhang, T. (2017). alpha7 nicotinic acetylcholine receptor agonist attenuates the cerebral injury in a rat model of cardiopulmonary bypass by activating the akt/GSK3beta pathway. *Mol Med Rep*, *16*(6), 7979–7986.

Tang, X., Di, X., & Liu, Y. (2017). Protective effects of donepezil against endothelial permeability. *Eur J Pharmacol*, *811*, 60–65.

Thrane, A. S., Rangroo Thrane, V., & Nedergaard, M. (2014). Drowning stars: Reassessing the role of astrocytes in brain edema. *Trends Neurosci*, *37*(11), 620–628.

Tran, K. A., Zhang, X., Predescu, D., Huang, X., Machado, R. F., Gothert, J. R., Malik, A. B., Valyi-Nagy, T., & Zhao, Y. Y. (2016). Endothelial beta-catenin signaling is required for maintaining adult blood-brain barrier integrity and Central nervous system homeostasis. *Circulation*, *133*(2), 177–186.

Van der, K. W. (2003). Loading and recycling of synaptic vesicles in the torpedo electric organ and the vertebrate neuromuscular junction. *ProgNeurobiol*, *71*, 269–303.

Vandeputte, C., Taymans, J. M., Casteels, C., Coun, F., Ni, Y., Van Laere, K., & Baekelandt, V. (2010). Automated quantitative gait analysis in animal models of movement disorders. *BMC Neuroscience*, *11*, 92.

Vlamings, R., Visser-Vandewalle, V., Koopmans, G., Joosten, E. A., Kozan, R., Kaplan, S., Steinbusch, H. W., & Temel, Y. (2007). High frequency stimulation of the subthalamic nucleus improves speed of locomotion but impairs forelimb movement in Parkinsonian rats. *Neuroscience*, *148*(3), 815–823.

Wang, W., Li, M., Wang, Y., Wang, Z., Zhang, W., Guan, F., Chen, Q., & Wang, J. (2017). GSK-3beta as a target for protection against transient cerebral ischemia. *Int J Med Sci*, *14*(4), 333–339.

Wang, Y., Bontempi, B., Hong, S. M., Mehta, K., Weinstein, P. R., Abrams, G. M., & Liu, J. (2008). A comprehensive analysis of gait impairment after experimental stroke and the therapeutic effect of environmental enrichment in rats. *J Cereb Blood Flow Metab*, *28*(12), 1936–1950.

Wang, Z. F., Wang, J., Zhang, H. Y., & Tang, X. C. (2008). Huperzine a exhibits anti-inflammatory and neuroprotective effects in a rat model of transient focal cerebral ischemia. *J Neurochem*, *106*(4), 1594–1603.

Yang, N. Y., Ding, C., Li, J., Zhang, Y., Xiang, R. L., Wu, L. L., Yu, G. Y., & Cong, X. (2017). Muscarinic acetylcholine receptor-mediated tight junction opening is involved in epiphora in late phase of submandibular gland transplantation. *J Mol Histol*, *48*(2), 99–111.

Yang, Y., & Rosenberg, G. A. (2011). Blood-brain barrier breakdown in acute and chronic cerebrovascular disease. *Stroke*, *42*(11), 3323–3328.

Zhao, Y., Dou, J., Luo, J., Li, W., Chan, H. H., Cui, W., Zhang, H., Han, R., Carlier, P. R., Zhang, X., & Han, Y. (2011). Neuroprotection against excitotoxic and ischemic insults by bis(12)-hupyridone, a novel anti-acetylcholinesterase dimer, possibly via acting on multiple targets. *Brain Res*, *1421*, 100–109.

Ziegler, N., Awwad, K., Fisslthaler, B., Reis, M., Devraj, K., Corada, M., Minardi, S. P., Dejana, E., Plate, K. H., Fleming, I., & Liebner, S. (2016). β-catenin is required for endothelial Cyp1b1 regulation influencing metabolic barrier function. *J Neurosci*, *36*(34), 8921–8935.

Zou, D., Luo, M., Han, Z., Zhan, L., Zhu, W., Kang, S., Bao, C., Li, Z., Nelson, J., Zhang, R., & Su, H. (2017). Activation of alpha-7 nicotinic acetylcholine receptor reduces brain edema in mice with ischemic stroke and bone fracture. *Mol Neurobiol*, *54*(10), 8278–8286.